Am J Cancer Res 2023;13(7):2841-2860
www.ajcr.us /ISSN:2156-6976/ajcr0150243

Original Article

Chinese herbal compound SanHuang decoction reverses axitinib resistance in ccRCC through regulating immune cell infiltration by affecting ADAMTS18 expression

Ben Xu, Jiaen Zhang, Lin Ye, Changwei Yuan

Department of Urology, Peking University First Hospital and Institute of Urology, Peking University, National Urological Cancer Center, Beijing, China

Received March 19, 2023; Accepted June 20, 2023; Epub July 15, 2023; Published July 30, 2023

Abstract: This investigation aims to study the reversal effect of the Chinese herbal compound SanHuang decoction on axitinib resistance in clear cell renal cell carcinoma (ccRCC) cells and its mechanistic role by employing cellular and mouse models. Axitinib-resistant ccRCC cell lines (A498-DR and 786-O-DR) were cultured and treated with SanHuang decoction. The apoptosis and migration of tumor cells were observed by flow cytometry and wound healing assays, respectively, and the expression of a disintegrin-like and metalloprotease with thrombospondin type 1 motif 18 (ADAMTS18) was evaluated by reverse transcription-polymerase chain reaction (RT-PCR) and Western blotting (WB). In addition, A498-DR cells were inoculated into mice to establish tumorigenic models, and the models were treated with normal saline, axitinib, or different concentrations of SanHuang decoction plus axitinib. Then, the tumor diameter in each group was measured, and the expression of ADAMTS18 was evaluated by RT-PCR, WB and immunohistochemistry. In addition, the distribution of T cells (CD45+, CD4+, CD8+) and PD-L1 expression was analyzed by flow cytometry to evaluate the level of immune cell infiltration. SanHuang decoction significantly reduced the proliferative activity of axitinib-resistant tumor cells and enhanced the sensitivity of tumors to axitinib *in vitro* (cell lines) and in mice. In the SanHuang decoction group, the expression level of ADAMTS18 was increased to some extent, and several phenomena were observed, including (1) subcutaneous transplanted tumors grew slower, (2) the CD45+/PD-L1 ratio was decreased and (3) the proportions of CD8+ and CD4+ T cells were increased. Overexpression of ADAMTS18 was synergistic with SanHuang decoction treatment to jointly improve tumor immune infiltration and inhibit immune escape. Pearson correlation analysis of sample data showed that there was a negative correlation between the expression of ADAMTS18 and PD-L1 in tumor tissues. In conclusion, the Chinese herbal compound SanHuang decoction can reverse axitinib resistance in ccRCC cells by regulating immune cell infiltration and affecting ADAMTS18 expression.

Keywords: SanHuang decoction, renal cell carcinoma, ADAMTS18, Chinese herbal compound, immune infiltration

Introduction

Clear cell renal cell carcinoma (ccRCC) is one of the most common urinary system malignancies and has the highest mortality rate. Despite early surgery in patients with localized ccRCC, recurrence and metastasis can occur in approximately 30% of cases [1]. ccRCC is less sensitive to traditional chemoradiotherapy, and there is a lack of effective treatment means for advanced patients. Since 2005, tyrosine kinase inhibitors (TKIs) such as axitinib have been widely applied to the clinical treatment of advanced ccRCC [2], and they have substantially extended the overall survival of patients and improved the disease control rate; they are recommended by urinary surgery guidelines as first-line drugs for the treatment of advanced ccRCC [3].

Approximately 1/3 of patients, however, have been found to be initially resistant to TKIs during clinical trials, and drug resistance can also emerge in initially sensitive patients after 1 year of medication, making it difficult for TKIs to effectively treat advanced ccRCC patients [4].

The mechanism of axitinib resistance in ccRCC remains unclear, and there are no efficient methods for reversing axitinib resistance. Therefore, it is of great importance to explore the mechanism of axitinib resistance in ccRCC and reverse this resistance using effective targets.

Natural medicine has multiple advantages in the treatment of malignancies. Through research on ancient books and modern documents, the special antitumor ability of curcumin has been found. According to relevant studies, curcumin can serve as a sensitizer for chemotherapeutic drugs or TKIs to reverse multidrug resistance by regulating the expression of different drug-resistant proteins [5, 6] and enhancing the chemotherapy sensitivity of lung cancer, colon cancer, pancreatic cancer, and breast cancer [7-10]. Recently, our research team reported for the first time throughout the world that curcumin can reverse sunitinib resistance in ccRCC cell lines *in vitro*, and its specific mechanism is presumably related to the regulation of disintegrin-like and metalloprotease with thrombospondin type 1 motif 18 (ADAMTS18) expression [11, 12]. Moreover, in 2022, we also identified that curcumin can inhibit the proliferation of ccRCC cells *in vitro* and *in vivo* by regulating miR-148/ADAMTS18 and suppressing autophagy [13].

To enhance the effect of curcumin, a Chinese herbal compound SanHuang decoction containing curcumin was prepared, and its reversal effect on axitinib resistance in ccRCC and specific mechanism were validated in cell lines and mice. To our knowledge, this is the first experiment to explore the mechanism of a Chinese herbal compound containing curcumin in reversing axitinib resistance in ccRCC in mice, which may provide novel insights for the treatment of advanced refractory ccRCC with integrated traditional and Western medicine in the future.

Methods

Drugs and reagents

Preparation of SanHuang decoction: 50 g of SanHuang crude herbs (30 g of *Astragalus membranaceus*, 10 g of prepared rhubarb, and 10 g of *Curcuma longa*) were extracted twice with distilled water (1:10, w/v) using reflux extraction, and the resulting liquid was preserved each time. The drug residues were then removed, and the remaining liquid from the two extractions was concentrated at 1 g/mL and filtered through a 0.2 μM filter (Millipore, Billerica, MA, USA). Finally, the extract was stored at -20°C. The above herbs were purchased from the Beijing Asian Games Village Hospital of Traditional Chinese Medicine.

ccRCC A498 and 786-O cell lines (Shanghai Institute of Cell Biology), axitinib (Beacon Pharma), curcumin (purity >98%, Shanghai PureOne Biotechnology), antibodies (Beijing Bioss Antibodies Co., Ltd.), polymerase chain reaction (PCR) kits (Thermo Fisher, USA), protein extraction kits (Thermo Fisher), RNA kits (Tiangen Biotech), electrophoresis apparatus and gel imaging system (Rio-Rad), Dulbecco's modified Eagle's medium (DMEM), and fetal bovine serum (Thermo Fisher) were used. All primers were designed by Sangon Biotech (Shanghai) Co., Ltd.

Construction of axitinib-resistant cell lines

A498 and 786-O cell lines were induced with axitinib at an initial concentration of 0.5 μM and cultured with new medium. After the cell lines became stable, the concentration of axitinib was increased by 0.5 μM each time until the cell lines became resistant to 15 μM axitinib (A498-DR and 786-O-DR).

Detection of apoptosis by flow cytometry

After the cell concentration was adjusted, the cells were cultured overnight. Following adherence to the wall, the cells were centrifuged for 48 h, washed twice with precooled phosphate-buffered saline (PBS), dispersed with 100 μL of binding buffer, and incubated with the corresponding dyes away from light at room temperature for 15 min. Then, 300 μL of binding buffer was added, and the cells were transferred to the corresponding flow tube away from light, followed by the detection of apoptosis.

Wound healing assay

After 24 h of culture, the cells were digested and suspended in serum-free medium. The cell concentration was adjusted, and the cells were inoculated into a 6-well plate. Upon reaching complete confluence, the cells were scratched vertically with a 200 μL pipette tip. The shed cells were washed away with PBS, and 2 mL of

serum-free medium was added for routine culture. At 0, 12, and 24 h after scratching, the cell scratch space was observed under an inverted microscope, and the relative scratch space was calculated ($space_{12 \text{ or } 24 \text{ h}}/space_{0 \text{ h}}$).

Reverse transcription-polymerase chain reaction (RT-PCR)

RNA was extracted from cells using RNA extraction kits. The target gene sequences were queried from the NCBI, and the primers were designed. The reaction conditions were as follows: 40 cycles × (95°C for 30 s, 95°C for 5 s, 60°C for 34 s, 70°C for 10 s, and 95°C for 15 s). Blank controls and internal reference controls were set up for amplification in the same system.

Western blotting (WB)

Total protein was extracted from cells, subjected to SDS-PAGE, transferred to a membrane at a constant current of 0.3 A for 2 h, blocked with 5% skim milk powder for 2 h, incubated with specific primary antibodies at 4°C overnight, washed 3 times with PBS (10 min/wash) and incubated with horseradish peroxidase (HRP)-labeled secondary antibodies for 2 h. Then, ECL substrate was added, the band was analyzed on a gel imaging system (Rio-Rad), and its gray value was calculated.

Axitinib-resistant animal models

This experiment was reviewed and approved by the Animal Ethics Committee (ethics No.: J2022023) of Peking University First Hospital on April 18th, 2022. BALB/c mice were purchased from Beijing Huafukang Biotechnology Co., Ltd. [license No. SCXK (Beijing) 2019-0008] and raised in an SPF laboratory. A498-DR cells were subcutaneously injected into the backs of mice. After tumor formation, the tumor was measured with a micrometer, and its volume was determined (L × W × H × 0.5). The tumor volume was measured every 2 days and is described as the mean ± standard deviation. When the volume reached approximately 80 mm^3, axitinib was administered by oral gavage (40 mg/kg/d). The tumor volume was monitored until drug resistance developed. The assessment for drug resistance was evaluated based on the increase in transplanted tumor volume >25% over the initial volume or continuous tumor growth during long-term observation.

The mice were randomly divided into 12 groups using a random number table (5 mice in each group) and administered the corresponding drugs by gavage for 30 days, and then the mice were euthanized. None of the mice died due to other unexpected causes. Animal health and behavior were monitored at least twice a day. After the experiment, euthanasia was performed by intraperitoneal injection of 100 mg/kg pentobarbital sodium. All animal welfare was fully considered, including efforts to minimize suffering and distress, use of analgesics or anesthetics, or special housing conditions. All of the research staff accepted special training in animal care and obtained the occupational qualification certificate for laboratory animals.

The detailed groups: 1) Control group: 53.6 mg/kg normal saline (morning) + 400 mg/kg normal saline (afternoon) + 400 mg/kg normal saline (evening); 2) Axitinib group: 53.6 mg/kg axitinib (morning) + 400 mg/kg normal saline (afternoon) + 400 mg/kg normal saline (evening); 3) Axitinib + SanHuang decoction (lower concentration) group: 53.6 mg/kg axitinib (morning) + 400 mg/kg SanHuang decoction (afternoon) + 400 mg/kg normal saline (evening); 4) Axitinib + SanHuang decoction (higher concentration) group: 53.6 mg/kg axitinib (morning) + 400 mg/kg SanHuang decoction (afternoon) + 400 mg/kg SanHuang decoction (evening); 5) Overexpressed-NC group: pADV-mCMV-3xFLAG-EGFP + 53.6 mg/kg normal saline (morning) + 400 mg/kg normal saline (afternoon) + 400 mg/kg normal saline (evening); 6) Overexpressed-ADAMTS18 group: pADV-mCMV-3xFLAG-EGFP-ADAMTS18 + 53.6 mg/kg normal saline (morning) + 400 mg/kg normal saline (afternoon) + 400 mg/kg normal saline (evening); 7) Overexpressed-ADAMTS18 + Axitinib group: pADV-mCMV-3xFLAG-EGFP-ADAMTS18 + 53.6 mg/kg axitinib (morning) + 400 mg/kg normal saline (afternoon) + 400 mg/kg normal saline (evening); 8) Overexpressed-ADAMTS18 + Axitinib + SanHuang decoction group: pADV-mCMV-3xFLAG-EGFP-ADAMTS18 + 53.6 mg/kg axitinib (morning) + 400 mg/kg SanHuang decoction (afternoon) + 400 mg/kg normal saline (evening); 9) shNC group: pADV-shRNA-Scramble + 53.6 mg/kg normal saline (morning) + 400 mg/kg normal saline (afternoon) + 400 mg/kg normal saline (evening); 10) shADAMTS18 group: pADV-ADAMTS18 shRNA + 53.6 mg/kg normal saline

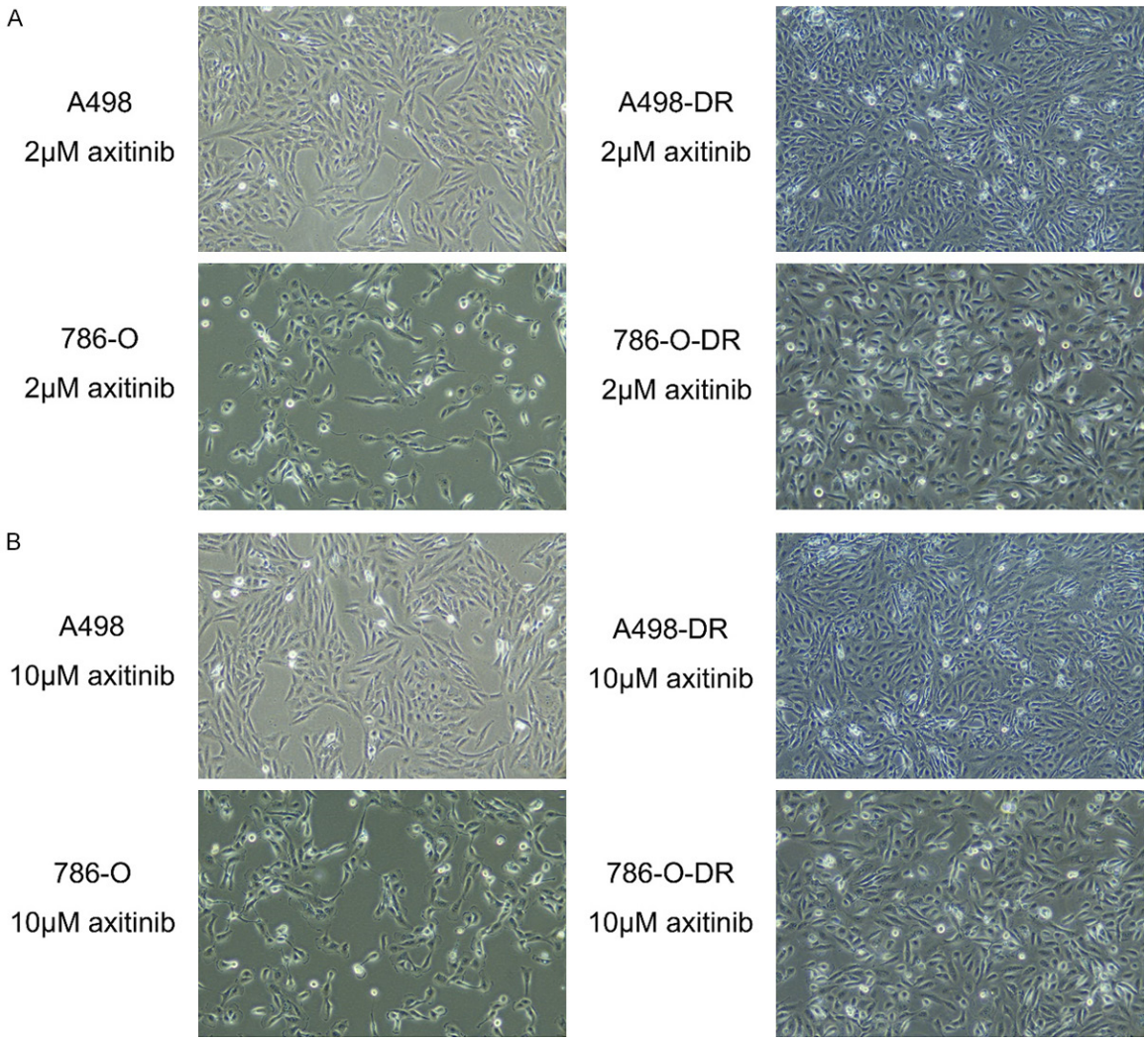

Figure 1. Axitinib-resistant cell lines. A: Low concentration (2 μM) of axitinib; B: High concentration (10 μM) of axitinib.

(morning) + 400 mg/kg normal saline (afternoon) + 400 mg/kg normal saline (evening); 11) shADAMTS18 + Axitinib group: pADV-ADAMTS18 shRNA + 53.6 mg/kg axitinib (morning) + 400 mg/kg normal saline (afternoon) + 400 mg/kg normal saline (evening); 12) shADAMTS18 + Axitinib + SanHuang decoction group: pADV-ADAMTS18 shRNA + 53.6 mg/kg axitinib (morning) + 400 mg/kg SanHuang decoction (afternoon) + 400 mg/kg normal saline (evening).

Analysis of T-cell subsets by flow cytometry (FCM)

The immunophenotypic analysis of tumor cells and single-cell suspensions was evaluated by FCM. All primary antibodies used in this study were purchased from BioLegend (CA, United States). CD45-APC-Cy7 (clone 30-F11), CD4-PE-Cy7 (clone RM4-4), CD8-FITC (clone 53-6.7), and PD-L1-PE (clone RMP1-30) were used for staining. For the analysis of cell apoptosis, according to the manufacturer's protocol, cells were stained with annexin V-fluorescein isothiocyanate (FITC) and propidium iodide (PI) (BD Apoptosis Detection Kit, BD Pharmangen, CA, United States). The fresh transplanted tumor tissue of the mouse model was cut into small pieces and then digested with type IV collagenase to produce a single cell suspension. After the single-cell suspension was filtered and washed with cold PBS, the cells and the primary antibody were coincubated on ice for 30 minutes. Then, they were washed and fixed in PBS containing 1% formalin. The data were ultimately analyzed by flow cytometry (CyAn ADP, Beckman) and FlowJo software.

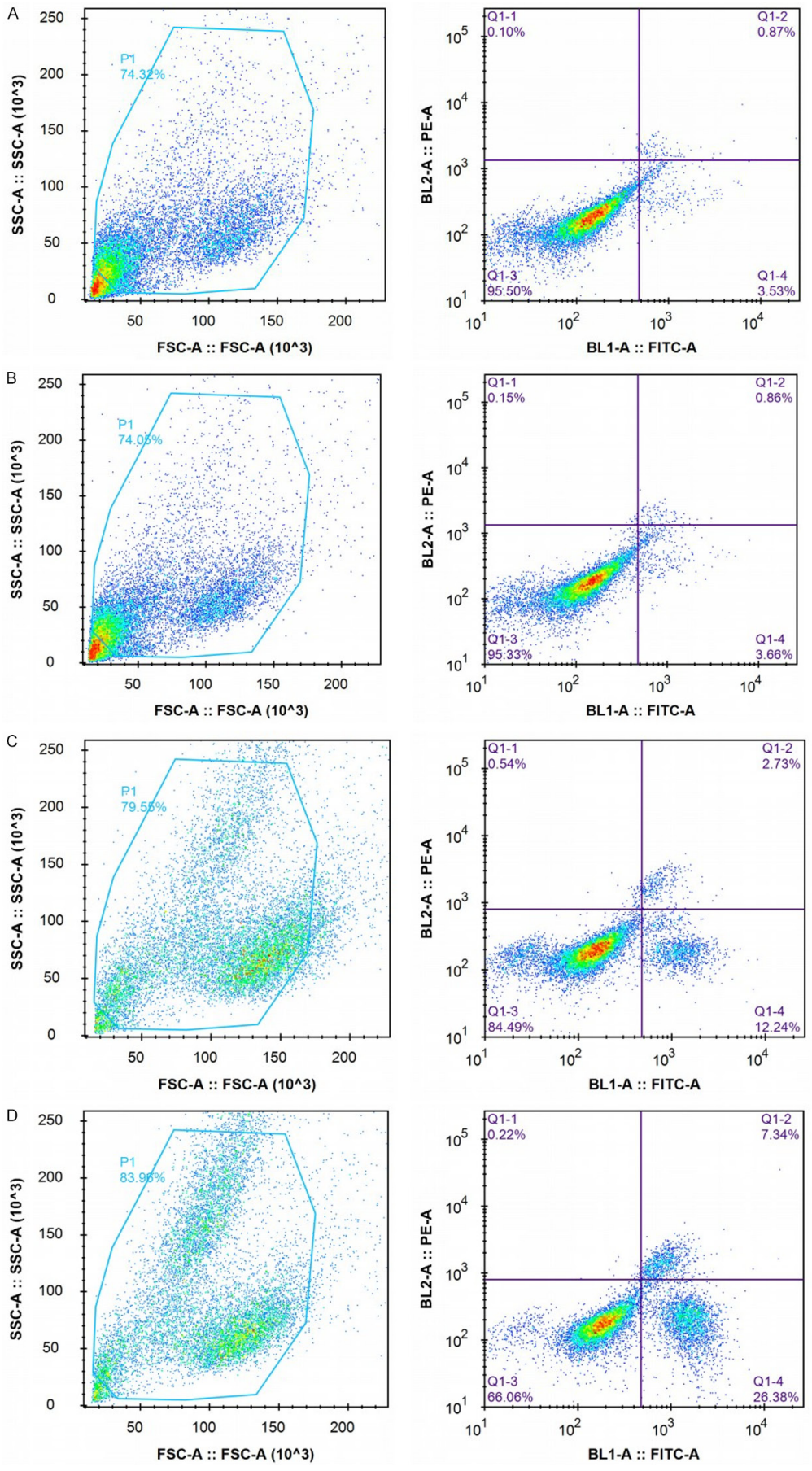
A
P1
74.32%
SSC-A :: SSC-A (10^3)
FSC-A :: FSC-A (10^3)
Q1-1
0.10%
Q1-2
0.87%
Q1-3
95.50%
Q1-4
3.53%
BL2-A :: PE-A
BL1-A :: FITC-A
B
P1
74.05%
SSC-A :: SSC-A (10^3)
FSC-A :: FSC-A (10^3)
Q1-1
0.15%
Q1-2
0.86%
Q1-3
95.33%
Q1-4
3.66%
BL2-A :: PE-A
BL1-A :: FITC-A
C
P1
79.55%
SSC-A :: SSC-A (10^3)
FSC-A :: FSC-A (10^3)
Q1-1
0.54%
Q1-2
2.73%
Q1-3
84.49%
Q1-4
12.24%
BL2-A :: PE-A
BL1-A :: FITC-A
D
P1
83.96%
SSC-A :: SSC-A (10^3)
FSC-A :: FSC-A (10^3)
Q1-1
0.22%
Q1-2
7.34%
Q1-3
66.06%
Q1-4
26.38%
BL2-A :: PE-A
BL1-A :: FITC-A

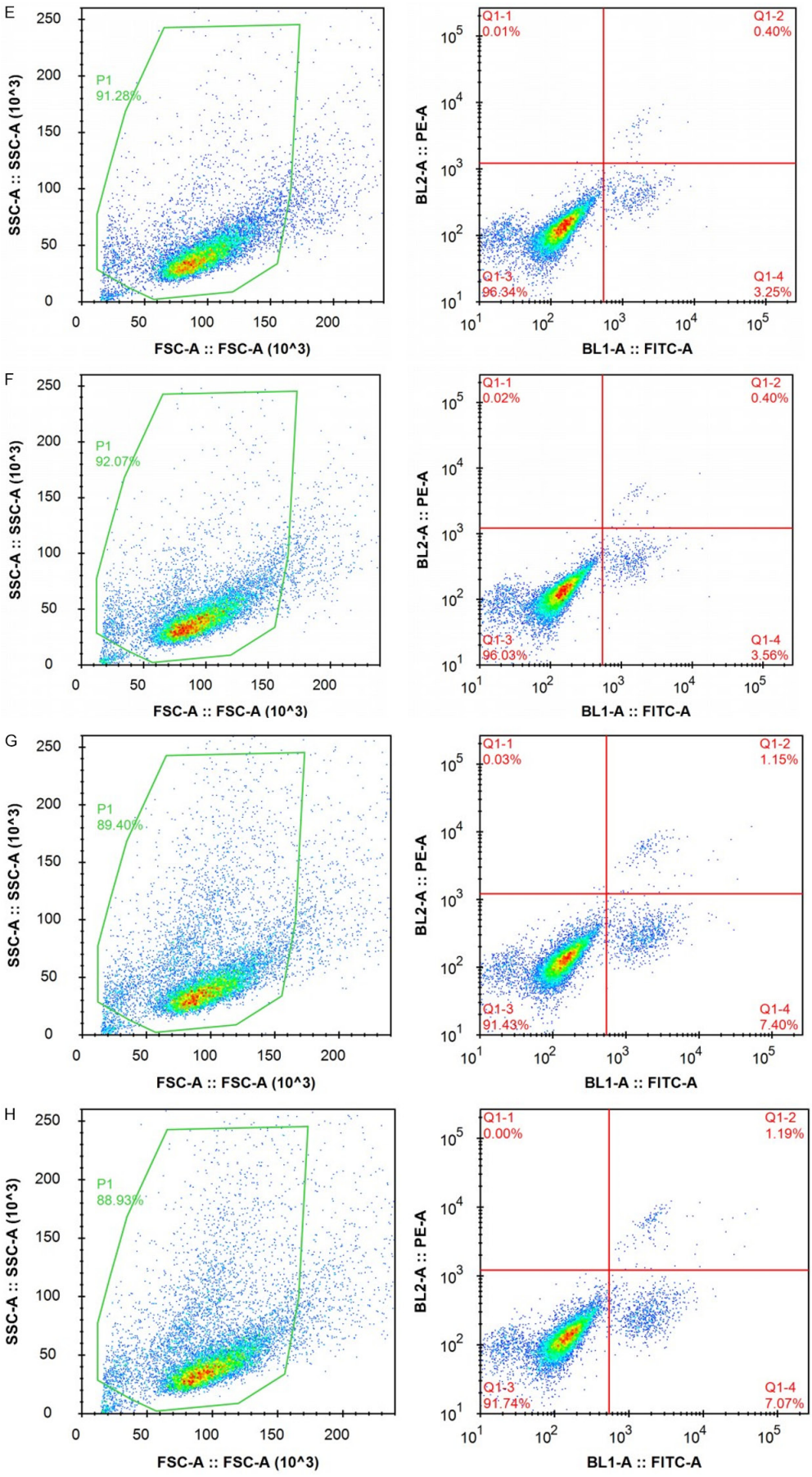
E
P1
91.28%
SSC-A :: SSC-A (10^3)
FSC-A :: FSC-A (10^3)
Q1-1
0.01%
Q1-2
0.40%
Q1-3
96.34%
Q1-4
3.25%
BL2-A :: PE-A
BL1-A :: FITC-A
F
P1
92.07%
SSC-A :: SSC-A (10^3)
FSC-A :: FSC-A (10^3)
Q1-1
0.02%
Q1-2
0.40%
Q1-3
96.03%
Q1-4
3.56%
BL2-A :: PE-A
BL1-A :: FITC-A
G
P1
89.40%
SSC-A :: SSC-A (10^3)
FSC-A :: FSC-A (10^3)
Q1-1
0.03%
Q1-2
1.15%
Q1-3
91.43%
Q1-4
7.40%
BL2-A :: PE-A
BL1-A :: FITC-A
H
P1
88.93%
SSC-A :: SSC-A (10^3)
FSC-A :: FSC-A (10^3)
Q1-1
0.00%
Q1-2
1.19%
Q1-3
91.74%
Q1-4
7.07%
BL2-A :: PE-A
BL1-A :: FITC-A

Figure 2. Cell apoptosis. A: A498-DR cells; B: A498-DR cells after treatment with 10 μM axitinib; C: A498-DR cells after treatment with 2 mg/mL SanHuang decoction; D: A498-DR cells after treatment with 10 mg/mL SanHuang decoction; E: 786-O-DR cells; F: 786-O-DR cells after treatment with 10 μM axitinib; G: 786-O-DR cells after treatment with 2 mg/mL SanHuang decoction; H: 786-O-DR cells after treatment with 10 mg/mL SanHuang decoction.

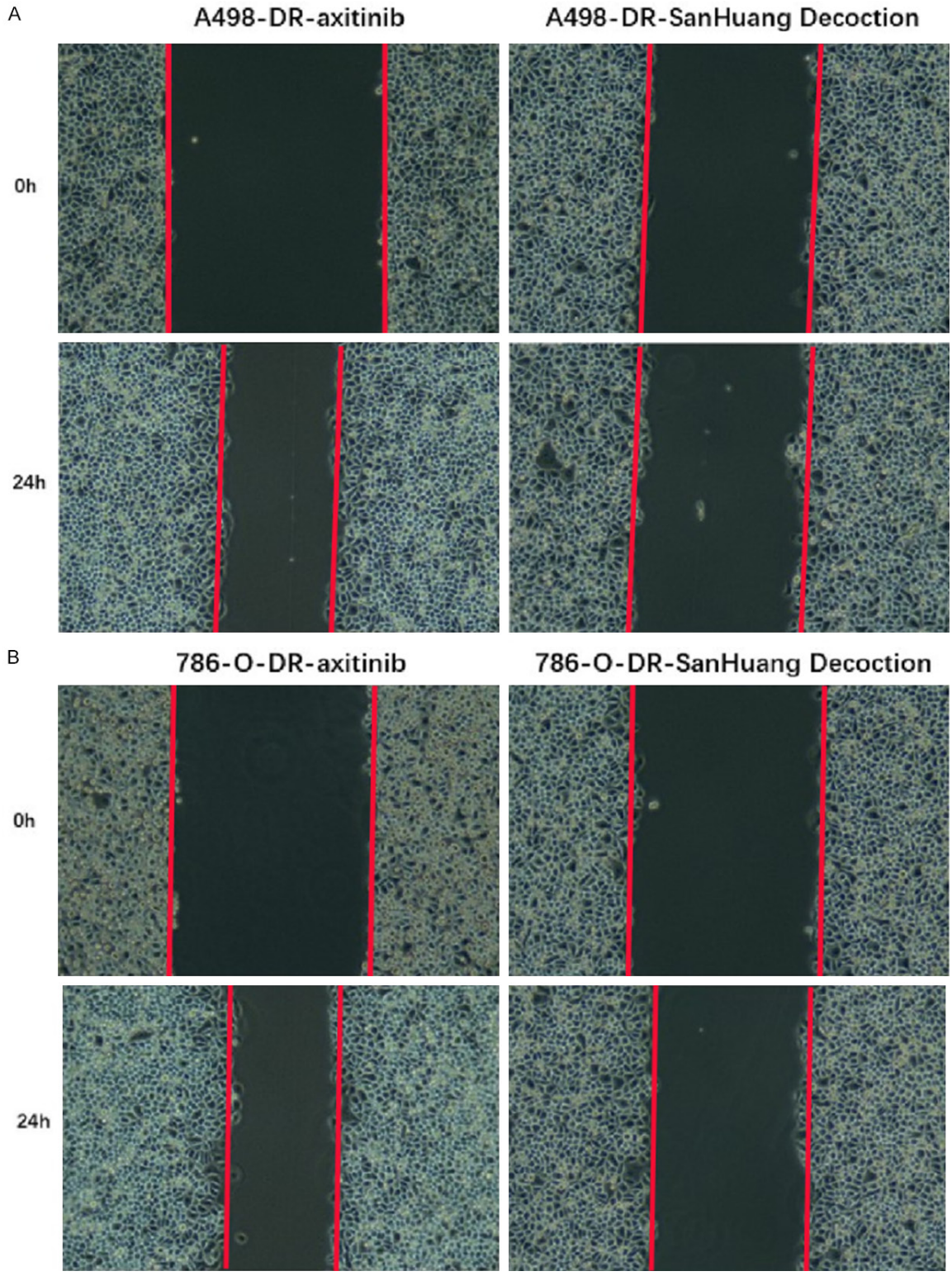

Figure 3. Wound healing assay. A: A498-DR cells; B: 786-O-DR cells.

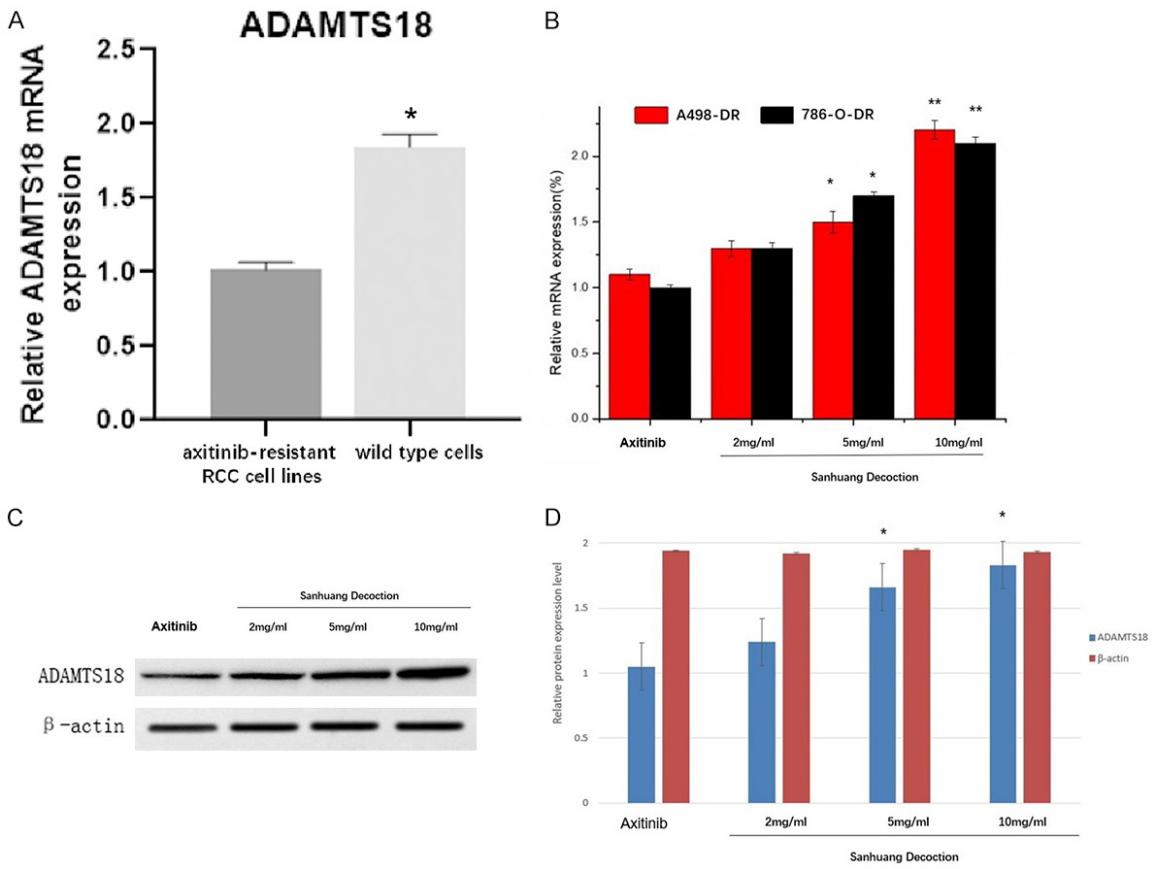

Figure 4. Expression of ADAMTS18 in cell lines. A. RT-PCR: Expression of ADAMTS18 in axitinib-resistant RCC cell lines and wild type cells; B. RT-PCR: Expression of ADAMTS18 in A498-DR and 786-O-DR cells after different treatments; C. WB: Expression of ADAMTS18 in A498-DR cells after different treatments; D. Histogram analysis of WB results.

Immunohistochemistry

The tumor tissue isolated from the killed mice was immediately fixed with 4% paraformaldehyde for 24 h and then embedded in paraffin. The embedded section was cut into 5 μm sections for staining. The dewaxed and rehydrated sections were boiled with sodium citrate antigen repair solution under high pressure for 3 minutes. After washing in PBS three times, the sections were incubated with 3% hydrogen peroxide methanol solution for 15 min to inhibit endogenous peroxidase activity. After blocking the nonspecific reaction with 10% normal rabbit serum, the sections were incubated with ADAMTS18 antibody at 4°C overnight. Then, the sections were washed and incubated with horseradish peroxidase-bound secondary antibody (GB23303, 1:200, Servicebio) at room temperature for 50 min and finally restained with hematoxylin.

Statistical analysis

Origin 8.5 was used for analysis. Measurement data are described as the mean ± standard deviation and were compared by *t* test between two groups and by one-way ANOVA combined with a post hoc Bonferroni test among groups. Enumeration data were described by percentages and compared by the chi-square test between two groups. $P<0.05$ was considered statistically significant.

Results

Successful construction of axitinib-resistant cell lines

The cell growth morphology was observed under an inverted microscope. Under low (2 μM) and high (10 μM) concentrations of axitinib, A498-DR and 786-O-DR cells displayed similar

A. overexpressed-ADAMTS18 group;
B. overexpressed-ADAMTS18 + Axitinib group;
C. overexpressed-ADAMTS18 + Axitinib + SanHuang Decoction group;
D. Axitinib group;
E. Axitinib+ SanHuang Decoction (lower concentration) group.

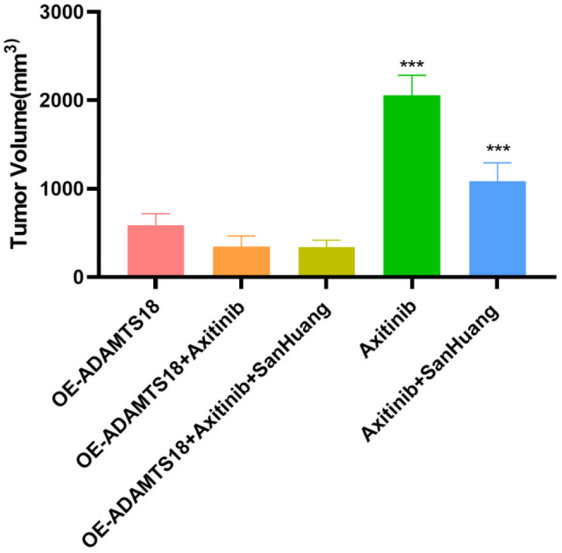

C

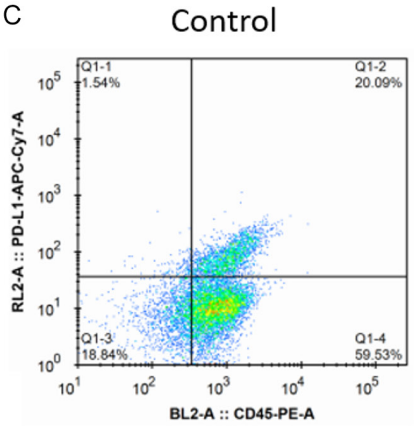

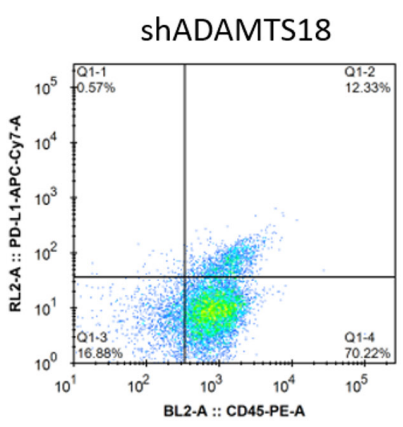

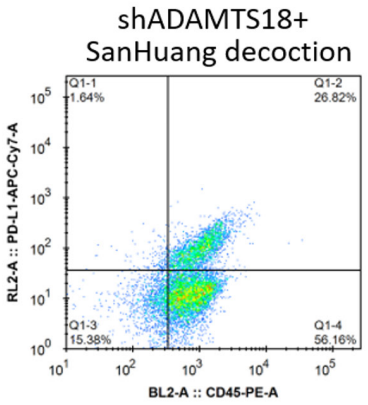

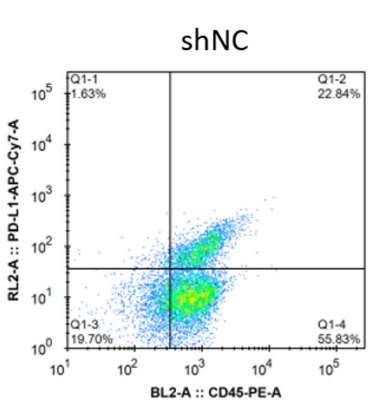

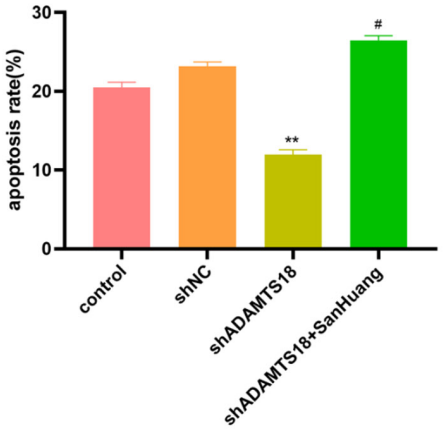

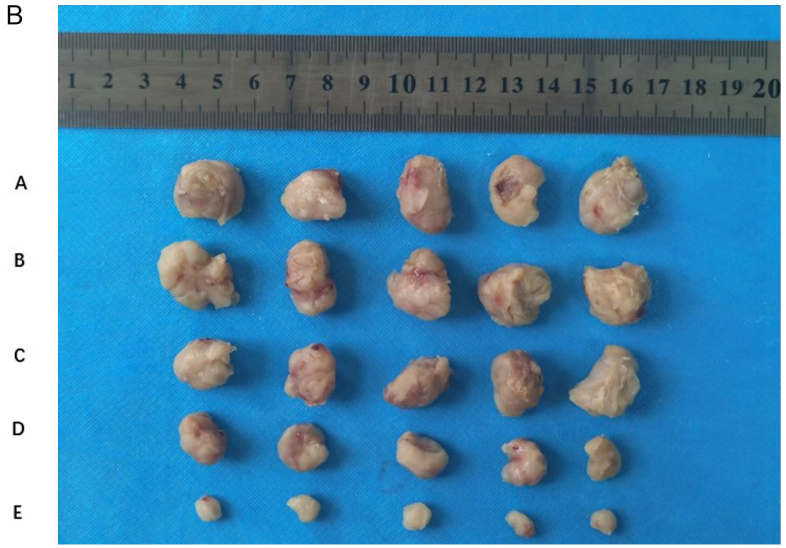

A. Control group;
B. shADAMTS18 group;
C. shADAMTS18 + Axitinib group;
D. shADAMTS18 + Axitinib + SanHuang Decoction group;
E. overexpressed-ADAMTS18 group.

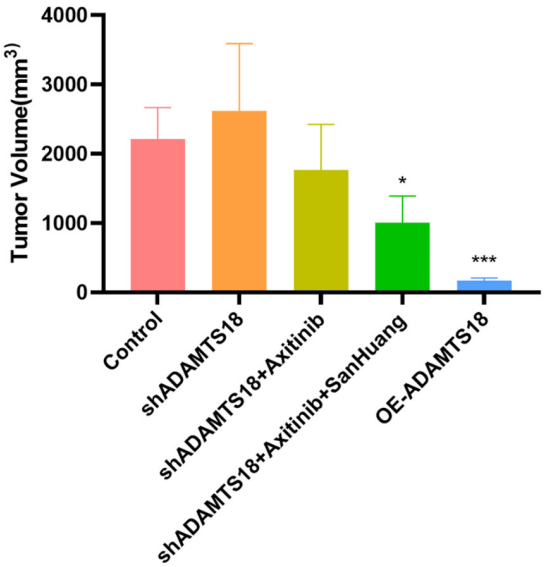

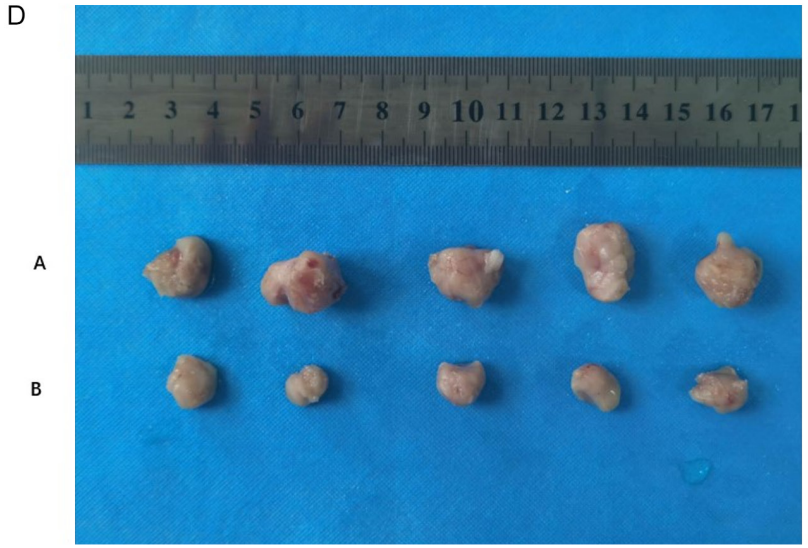

A. Axitinib+ SanHuang Decoction (lower concentration) group;
B. Axitinib+ SanHuang Decoction (higher concentration) group.

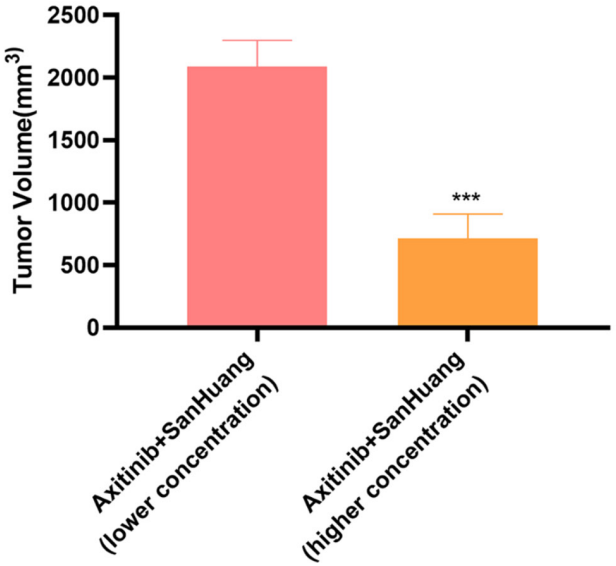

Figure 5. SanHuang decoction inhibited axitinib-resistant tumor growth in BALB/c mice. A: Tumor volume in different groups; B: Tumor volume in different groups; C: The apoptosis rate of tumor in different groups; D: Tumor volume in different concentrations of SanHuang decoction group.

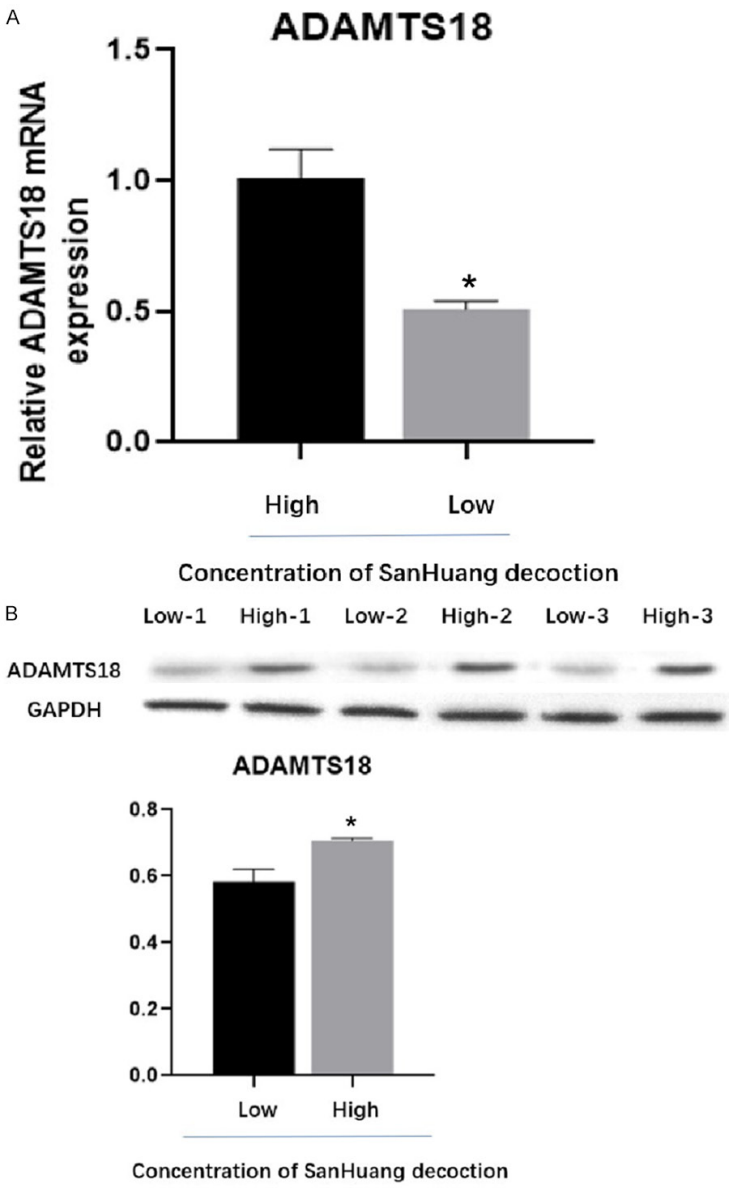

Figure 6. Expression of ADAMTS18 after SanHuang decoction treatment in BALB/c mice. A: RT-PCR: Expression of ADAMTS18 in different concentrations of SanHuang decoction group; B: WB: Expression of ADAMTS18 in different concentrations of SanHuang decoction group.

changes (*i.e.*, spindle-shaped and clustered growth), while A498 and 786-0 cells showed dispersed growth (**Figure 1A**, **1B**).

Axitinib plus SanHuang decoction could induce apoptosis similar to axitinib in wild-type cells

The apoptosis rate of A498-DR cells had no significant changes under 10 μM axitinib (**Figure 2A**, **2B**), while the apoptosis rate was significantly increased under low (2 mg/mL) (**Figure 2C**) and high (10 mg/mL) concentrations of SanHuang decoction combined with 10 μM axitinib (**Figure 2D**). For A498-DR cells, 10 μM axitinib plus 2 mg/mL SanHuang decoction induced apoptosis similar to axitinib in wild-type cells. Similar results were also observed in the 786-0-DR cell line. The apoptosis rate of 786-0-DR cells had no significant changes under 10 μM axitinib (**Figure 2E**, **2F**), while the apoptosis rate was increased under low (2 mg/mL) (**Figure 2G**) and high (10 mg/mL) concentrations of SanHuang decoction combined with 10 μM axitinib (**Figure 2H**).

Axitinib plus SanHuang decoction inhibited cell migration as well as axitinib in wild-type cells

The results of the wound healing assay showed that the relative scratch space of A498-DR and 786-0-DR cells at 24 h was significantly increased in the SanHuang decoction + axitinib group compared to the axitinib group, and the difference was statistically significant (**Figure 3A**, **3B**).

The reversal effect of SanHuang decoction on drug resistance in cell lines in vitro might be related to the regulation of ADAMTS18

The results of RT-PCR analysis showed that the expression level of ADAMTS18 was higher in wild-type cells than in axitinib-resistant ccRCC cell lines (**Figure 4A**). After treatment with SanHuang decoction, the expression level of ADAMTS18 was increased in A498-DR and 786-0-DR cells, and there were statistically significant differences under 5 mg/mL and 10 mg/mL SanHuang decoction (**Figure 4B**). A sim-

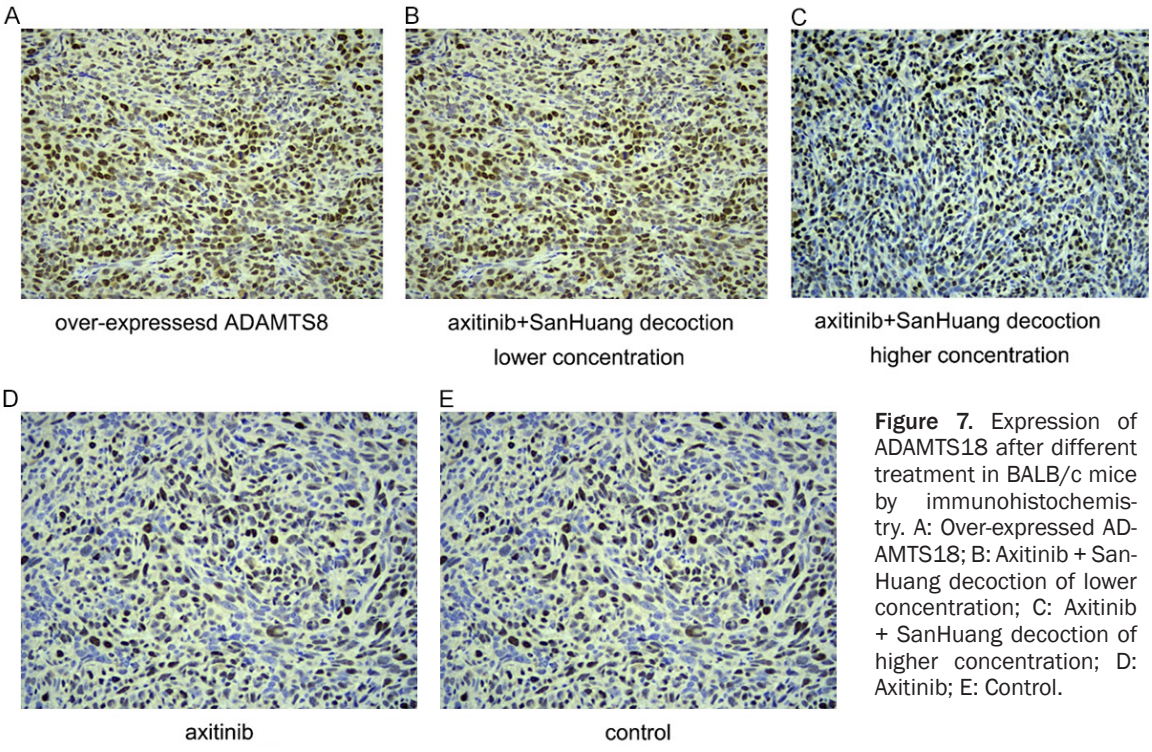

Figure 7. Expression of ADAMTS18 after different treatment in BALB/c mice by immunohistochemistry. A: Over-expressed ADAMTS18; B: Axitinib + SanHuang decoction of lower concentration; C: Axitinib + SanHuang decoction of higher concentration; D: Axitinib; E: Control.

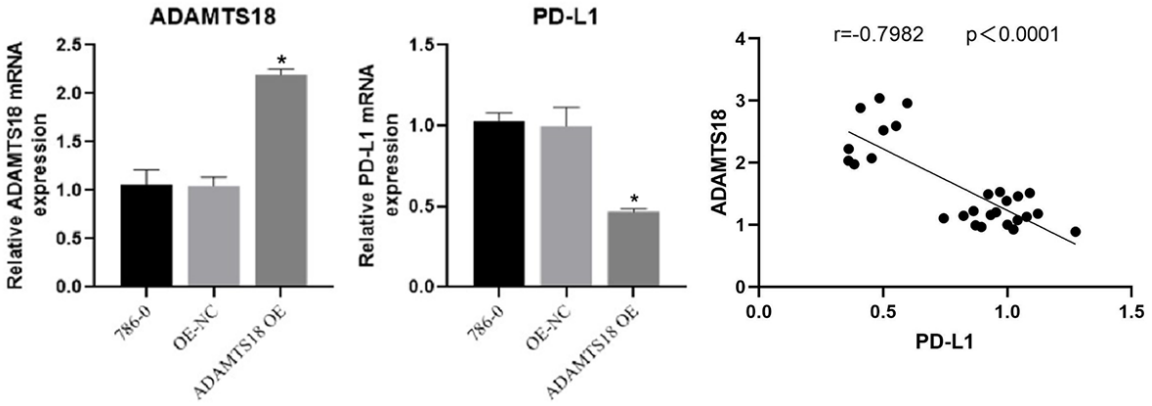

Figure 8. The relationship between ADAMTS18 and PD-L1.

ilar trend was observed in A498-DR cells by WB (**Figure 4C**, **4D**).

SanHuang decoction could suppress axitinib-resistant tumor growth in BALB/c mice

BALB/c mice were treated with axitinib 13 d after subcutaneous tumor formation. The tumor began to develop resistance to axitinib, and its volume was significantly expanded from the 20th d, indicating drug resistance. According to the *in vivo* tumor size analysis (**Figure 5A**, **5B**), the combination of SanHuang decoction and axitinib could further reduce the tumor volume, suggesting that SanHuang decoction reversed axitinib drug resistance in BALB/c mice. Simultaneously, when the ADAMTS18 gene was overexpressed/silenced, the tumor volume of mice was significantly reduced/increased, denoting that the ADAMTS18 gene may also reverse axitinib resistance in tumor cells. When ADAMTS18 was overexpressed, external addition of SanHuang decoction did not further enhance the decreased tumor vol-

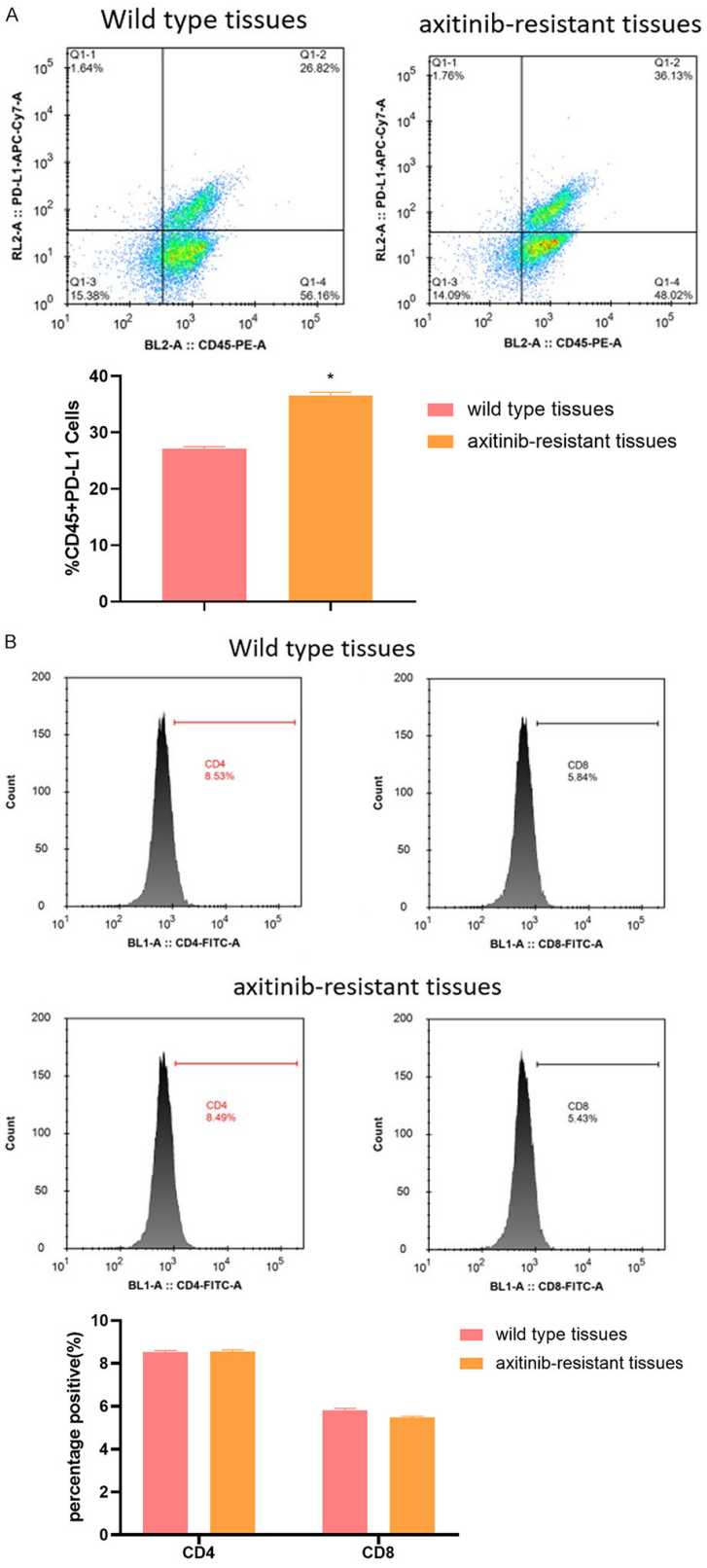

Figure 9. The immune cell infiltration in wild type tissues and axitinib-resistant tissues. A: The level of CD45+/PD-L1 in different groups; B: The level of CD8+ and CD4+ T cells in different groups.

ume, which denoted that overexpression of ADAMTS18 could fully reverse the role of SanHuang decoction in sensitizing axitinib, and in other words, SanHuang decoction played the role of suppressing tumor growth mainly through regulating ADAMTS18 expression. It could also be determined from the apoptosis analysis that silenced ADAMTS18 might inhibit the apoptosis of tumor cells, but this process could be reversed by the use of SanHuang decoction (**Figure 5C**). Further comparing the effects of different administrations of SanHuang decoction on tumors in mice, the results showed that the tumor volume of the once a day group was significantly larger than that of the twice a day group, suggesting that the reversal of axitinib resistance by SanHuang decoction was dose-dependent (**Figure 5D**).

The reversal of axitinib-resistant tumor growth by SanHuang decoction might be regulated by ADAMTS18

The tumor tissues of three mice in the "axitinib + SanHuang decoction (lower concentration) group" and "axitinib + SanHuang decoction (higher concentration) group" were collected for RT-PCR and WB detection. The results showed that the mRNA expression level of the ADAMTS18 gene in the high concentration group was higher than that in the low concentration group (**Figure 6A**), with similar conclusions at the protein expression level (**Figure 6B**). The immunohistochemical results also showed that the ADAMTS18 gene expression level in the SanHuang

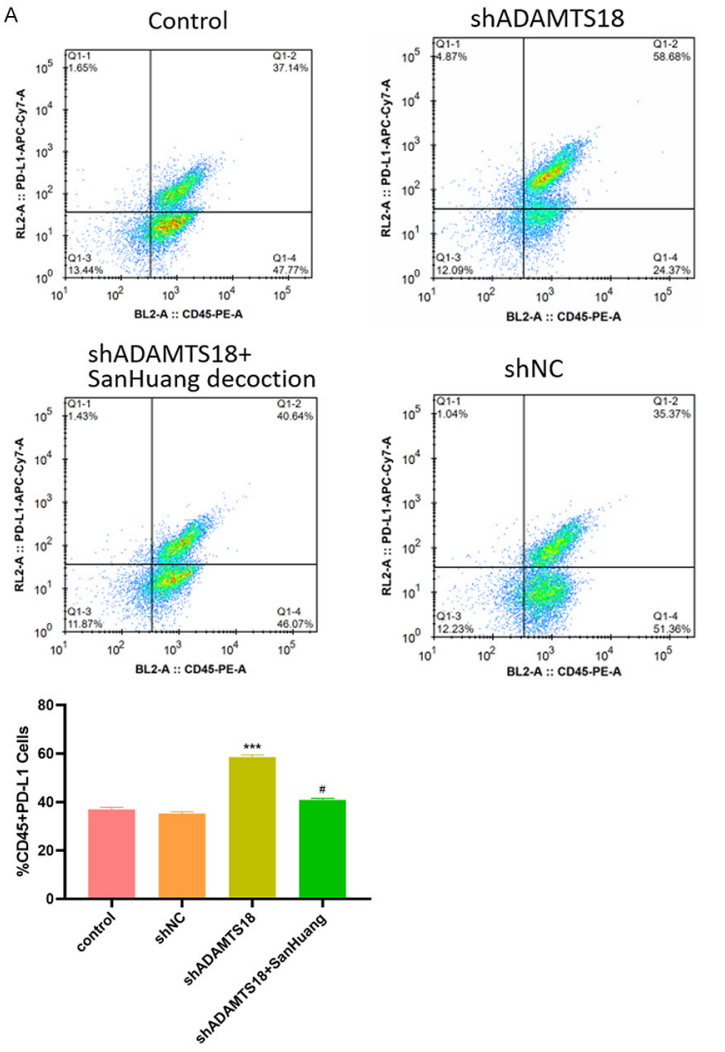

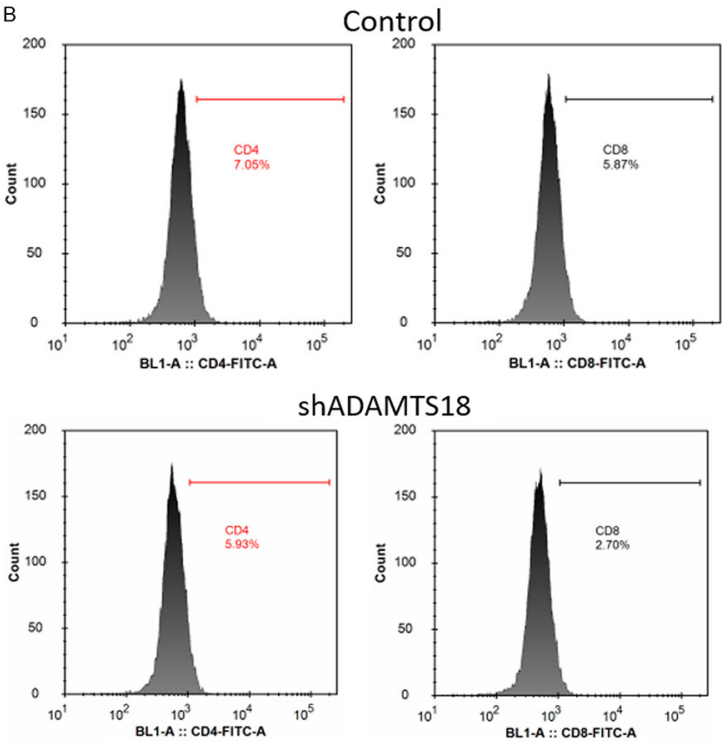

decoction treatment group was higher than that in the group without SanHuang decoction (**Figure 7A-E**).

SanHuang decoction might reverse axitinib resistance in ccRCC by regulating immune cell infiltration and affecting ADAMTS18 expression

The levels of ADAMTS18 and PD-L1 in the ADAMTS18-overexpressing group of mouse tumor tissues were analyzed by qRT-PCR. Pearson correlation analysis showed that the expression of ADAMTS18 and PD-L1 was negatively correlated (**Figure 8**). Therefore, it was concluded that PD-L1 might be the potential regulatory target of ADAMTS18, and the regulatory effect of SanHuang decoction on ADAMTS18 might influence the expression level of PD-L1 by affecting the infiltration state of immune cells.

The cell suspension was prepared from the transplanted tumor tissue of mice and stained with CD45-, CD4-, CD8-, and PD-L1-specific antibodies. The stained cells were analyzed by flow cytometry. The immune cell infiltration in wild-type tissues and axitinib-resistant tissues was first compared in **Figure 9A**, **9B**. Subsequently, the results showed that compared with that in the control group, the CD45+/PD-L1 ratio in the shADAMTS18 group was increased (**Figure 10A**), with a reduction in the proportion of CD8+ and CD4+ T cells (**Figure 10B**, **10C**), denoting that tumor immune infiltration was decreased and immune escape was promoted. However, by using SanHuang decoction, the above phenomenon could be reversed (**Figure 10A-C**). Compared with the low concentration SanHuang decoction group, the high concentration SanHuang decoction group exhibited a decreased

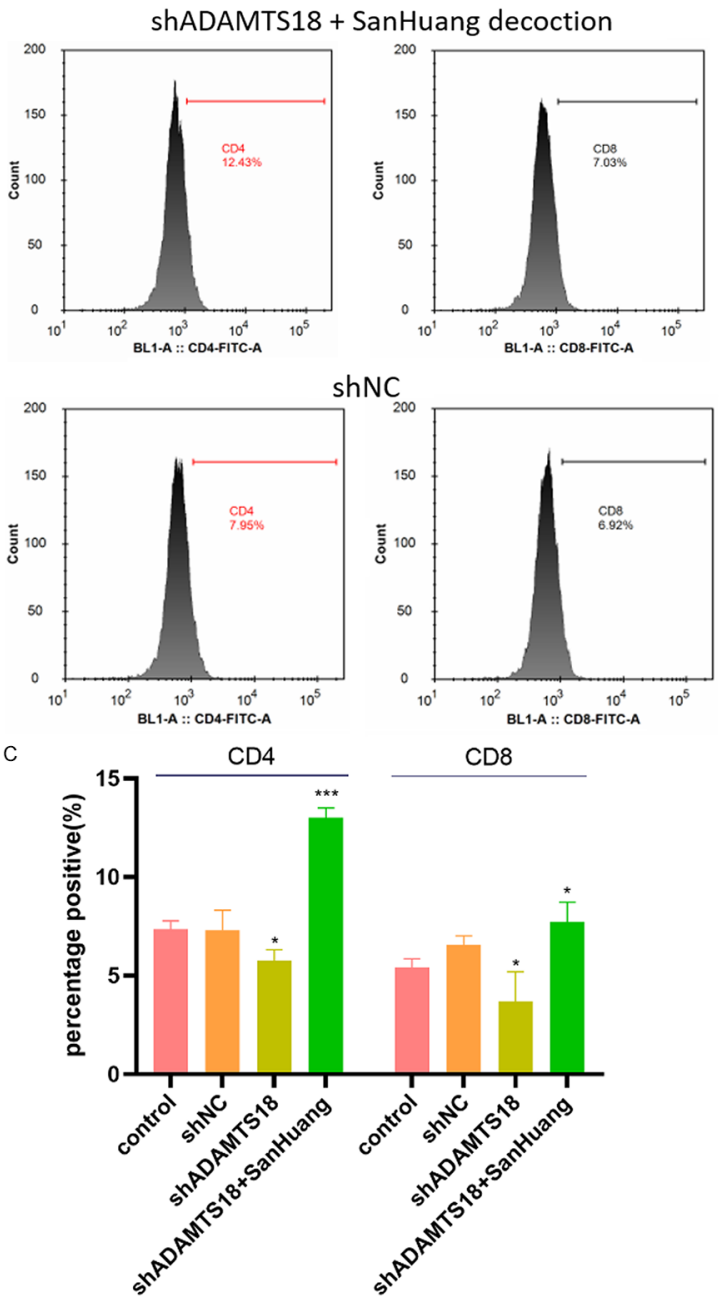

Figure 10. The analysis of immune cell infiltration. A: The level of CD45+/PD-L1 in different groups; B: The level of CD8+ and CD4+ T cells in different groups; C: Histogram analysis of FCM results.

CD45+/PD-L1 ratio and an increases proportion of CD8+ and CD4+ T cells (**Figure 11A-D**).

Similarly, compared with the control group, the CD45+/PD-L1 ratio in the ADAMTS18-overexpressing group was decreased (**Figure 12A**), with an increasing proportion of CD8+ and CD4+ T cells (**Figure 12B**, **12C**). Simultaneously, by using SanHuang decoction, the above pattern could be further promoted (**Figure 12A-C**).

Discussion

Axitinib, currently the major drug for the treatment of ccRCC, can greatly improve the survival status of ccRCC patients compared with that of patients treated with classic cytokine drugs, with the overall survival extended 19-26 months [14, 15]. With the popularization and application of axitinib, however, drug resistance has gradually developed and even worsened with prolonged administration time. Therefore, reducing the drug resistance of axitinib and improving its potency has become a research focus.

As a traditional Chinese herb, curcumin exerts an inhibitory effect on a variety of tumors. However, curcumin is a monomer of a traditional Chinese herb with a single mechanism, restricting its use in conventional anticancer therapy. The SanHuang decoction used in this study is a traditional Chinese herbal compound containing curcumin, created by Professor Xu ZY, a famous doctor of traditional Chinese medicine in Jiangsu, China, and prepared using *Astragalus membranaceus*, prepared rhubarb and *Curcuma longa* at 3:1:1 ratio [16]. It has been applied for 4 decades in clinical trials, and its use in breast cancer has even become popular since it can improve the inflammatory microenvironment and enhance the chemotherapy sensitivity of breast cancer [17, 18]. As proven by basic research, the mechanism by which SanHuang decoction regulates resistance to Western medicine may be related to the PI3K/AKT signaling pathway [19-24]. Our team had already reported for the first time that curcumin can affect the AKT signaling pathway by regulating ADAMTS18, thereby suppressing the development of ccRCC [12,

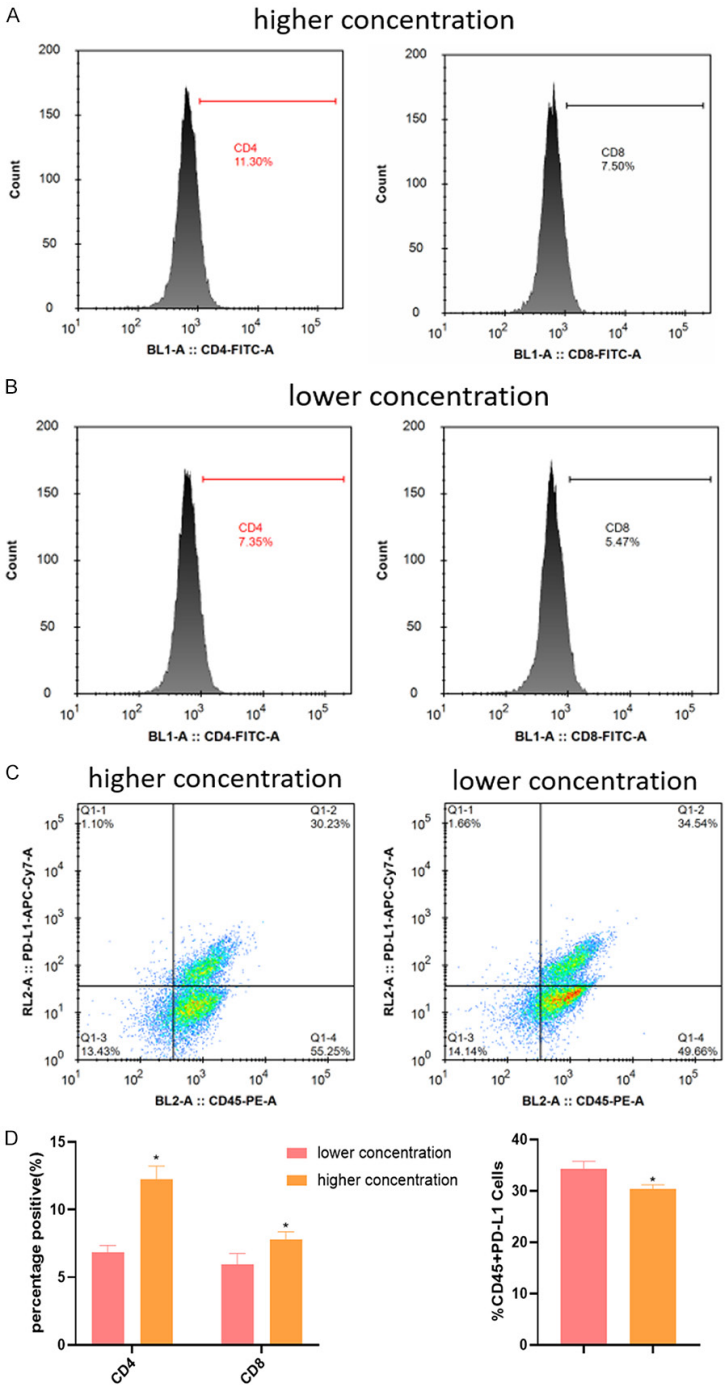

Figure 11. The analysis of CD45+/PD-L1, CD8+ and CD4+ T cells in different concentrations of SanHuang decoction treatment. A: The level of CD8+ and CD4+ T cells in higher concentration; B: The level of CD8+ and CD4+ T cells in lower concentration; C: The level of CD45+/PD-L1 in different groups; D: Histogram analysis of FCM results.

13] and reversing the drug resistance of tyrosine kinase inhibitors to ccRCC [11]. Therefore, it is inferred that SanHuang decoction containing curcumin may also affect the AKT signaling pathway by regulating ADAMTS18, thereby inhibiting ccRCC and reversing drug resistance.

In this experiment, the above conclusion was first verified *in vitro* using cell lines and then verified *in vivo* using a mouse animal model. Verification using mice was the highlight of this experiment. A498-DR was subcutaneously injected into mice to successfully establish axitinib-resistant model animals. It was found that the overall tumor volume was reduced in the SanHuang decoction group, and that it was more significantly reduced in the SanHuang group compared to the axitinib group, indicating that SanHuang decoction can enhance sensitivity to axitinib. In terms of the molecular biological mechanism, SanHuang decoction could increase the level of ADAMTS18 in tumor tissues. It was discovered by our team for the first time that ADAMTS18 is a tumor suppressor gene in ccRCC, and its low expression can contribute to the occurrence and development of ccRCC [25, 26]. In this experiment, SanHuang decoction promoted the recovery of ADAMTS18 expression in drug-resistant ccRCC cell lines *in vitro* and *in vivo*. Therefore, it is inferred that the reversal effect of SanHuang decoction on axitinib resistance is possibly related to the regulation of ADAMTS18.

According to previous studies, the upregulated expression of PD-L1 in tumor or interstitial cells is the basic mechanism to promote host immune evasion in tumor cells [27]. Tumor cells can inhibit the proliferation of T lymphocytes, especially CD8+ T lymphocytes, through the PD-L1/PD-1 pathway [28]. PD-L1 blockade can alleviate immunosuppression, enhance antitumor immunity, and cause ex-

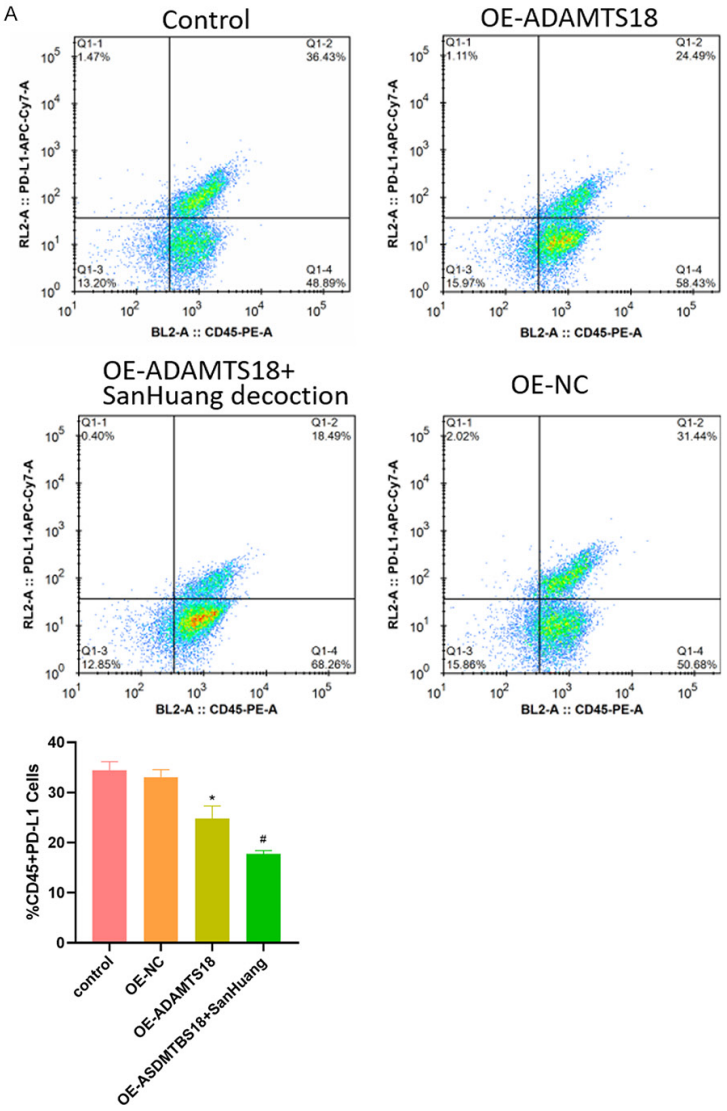

pansion of tumor-infiltrating lymphocytes [29]. It has been suggested that PD-L1 is mainly expressed on activated peripheral CD4+ T cells, CD8+ T cells and B cells [30]. Nevertheless, traditional PD1/PD-L1 immunosuppressants are expensive and cause large adverse reactions. It is difficult to popularize this type of therapy in developing countries such as China. Therefore, it is essential to find a drug that can play a similar role in blocking PD1/PD-L1.

In this study, it was found that when ADAMTS18 was knocked out, some phenomena were observed, including (1) the subcutaneously transplanted tumor in mice grew faster, (2) the CD45+/PD-L1 ratio was increased, and (3) the proportions of CD8+ and CD4+ T cells were decreased. After treatment with SanHuang decoction, compared with the shADAMTS18 group, the biological effect of transplanted tumors was completely opposite. The above results suggest that the deletion of ADAMTS18 further reduces the tumor infiltration of CD8+ and CD4+ cytotoxic T lymphocytes, while treatment with SanHuang decoction has the opposite effect. Although many studies have clarified that ADAMTS18 has abnormal expression in different tumor cells [31, 32], there are still no reports about ADAMTS18 and immune infiltration. In this research, it was found for the first time that silencing ADAMTS18 in ccRCC tissue is related to inhibiting the cytotoxic infiltration of CD4+ and CD8+ T lymphocytes, while overexpression of the ADAMTS18 gene has a synergistic effect with the treatment of SanHuang decoction, which may play a similar role as an immunosuppressive agent, improving tumor immune infiltration and inhibiting immune escape by affecting the expres-

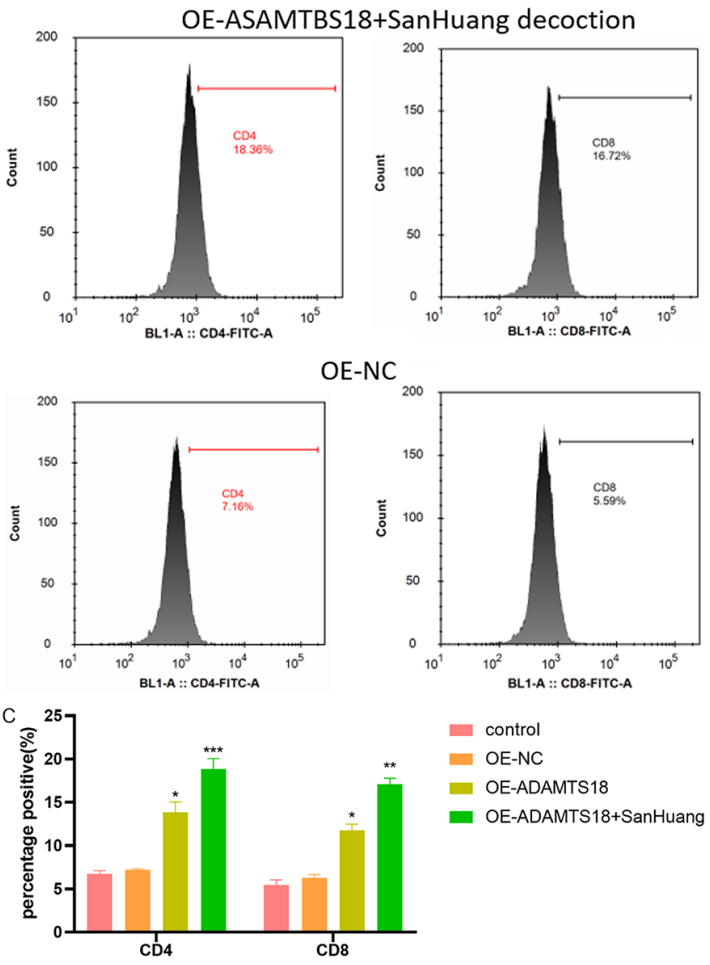

Figure 12. The analysis of immune cell infiltration. A: The level of CD45+/PD-L1 in different groups; B: The level of CD8+ and CD4+ T cells in different groups; C: Histogram analysis of FCM results.

sion of ADAMTS18 and PD-L1. Correlation analysis also showed that the expression of ADAMTS18 and PD-L1 was negatively correlated.

In conclusion, the Chinese herbal compound SanHuang decoction can reverse axitinib resistance in ccRCC cells by regulating immune cell infiltration and affecting ADAMTS18 expression.

Acknowledgements

This study was supported by grants from National Natural Science Foundation of China (No. 82200740) and Beijing Traditional Chinese Medicine Development Foundation (No. QN-2020-03).

Disclosure of conflict of interest

None.

Address correspondence to: Ben Xu, Department of Urology, Peking University First Hospital and Institute of Urology, Peking University, National Urological Cancer Center, No. 8 Xishiku Street, Xicheng District, Beijing 100034, China. Tel: +86-10-83572418; Fax: +86-10-66175710; E-mail: xuben_pku@sina.com

References

[1] Capitanio U and Montorsi F. Renal cancer. Lancet 2016; 387: 894-906.

[2] Lalani AA, McGregor BA, Albiges L, Choueiri TK, Motzer R, Powles T, Wood C and Bex A. Systemic treatment of metastatic clear cell renal cell carcinoma in 2018: current paradigms, use of immunotherapy, and future directions. Eur Urol 2019; 75: 100-110.

[3] Ljungberg B, Albiges L, Abu-Ghanem Y, Bensalah K, Dabestani S, Fernández-Pello S, Giles RH, Hofmann F, Hora M, Kuczyk MA, Kuusk T, Lam TB, Marconi L, Merseburger AS, Powles T, Staehler M, Tahbaz R, Volpe A and Bex A. European Association of Urology guidelines on renal cell carcinoma: the 2019 update. Eur Urol 2019; 75: 799-810.

[4] Powles T, Staehler M, Ljungberg B, Bensalah K, Canfield SE, Dabestani S, Giles R, Hofmann F, Hora M, Kuczyk MA, Lam T, Marconi L, Merseburger AS, Volpe A and Bex A. Updated EAU guidelines for clear cell renal cancer patients who fail VEGF targeted therapy. Eur Urol 2016; 69: 4-6.

[5] Wen C, Fu L, Huang J, Dai Y, Wang B, Xu G, Wu L and Zhou H. Curcumin reverses doxorubicin resistance via inhibition the efflux function of $ABCB_4$ in doxorubicin-resistant breast cancer cells. Mol Med Rep 2019; 19: 5162-5168.

[6] Tan BL and Norhaizan ME. Curcumin combination chemotherapy: the implication and efficacy in cancer. Molecules 2019; 24: 2527.

[7] Chen P, Huang HP, Wang Y, Jin J, Long WG, Chen K, Zhao XH, Chen CG and Li J. Curcumin

overcome primary gefitinib resistance in non-small-cell lung cancer cells through inducing autophagy-related cell death. J Exp Clin Cancer Res 2019; 38: 254.
[8] Mbese Z, Khwaza V and Aderibigbe BA. Curcumin and its derivatives as potential therapeutic agents in prostate, colon and breast cancers. Molecules 2019; 24: 4386.
[9] Yoshida K, Toden S, Ravindranathan P, Han HY and Goel A. Curcumin sensitizes pancreatic cancer cells to gemcitabine by attenuating PRC2 subunit EZH2, and the lncRNA PVT1 expression. Carcinogenesis 2017; 38: 1036-1046.
[10] Luo H, Vong CT, Chen H, Gao Y, Lyu P, Qiu L, Zhao M, Liu Q, Cheng Z, Zou J, Yao P, Gao C, Wei J, Ung COL, Wang S, Zhong Z and Wang Y. Naturally occurring anti-cancer compounds: shining from Chinese herbal medicine. Chin Med 2019; 14: 48.
[11] Xu B, Zhu WJ, Peng YJ and Cheng SD. Curcumin reverses the sunitinib resistance in clear cell renal cell carcinoma (ccRCC) through the induction of ferroptosis via the ADAMTS18 gene. Transl Cancer Res 2021; 10: 3158-3167.
[12] Xu B, Peng YJ and Zhu WJ. Curcumin inhibits viability of clear cell renal cell carcinoma by down-regulating ADAMTS18 gene methylation though NF-kB and AKT signaling pathway. Chin J Integr Med 2022; 28: 419-424.
[13] Xu B, Yuan CW and Zhang JE. Curcumin inhibits proliferation of renal cell carcinoma in vitro and in vivo by regulating miR-148/ADAMTS18 through suppressing autophagy. Chin J Integr Med 2022; [Epub ahead of print].
[14] Rini BI, Halabi S, Rosenberg JE, Stadler WM, Vaena DA, Ou SS, Archer L, Atkins JN, Picus J, Czaykowski P, Dutcher J and Small EJ. Bevacizumab plus interferon alfa compared with interferon alfa monotherapy in patients with metastatic renal cell carcinoma: CALGB 90206. J Clin Oncol 2008; 26: 5422-5428.
[15] Escudier B, Pluzanska A, Koralewski P, Ravaud A, Bracarda S, Szczylik C, Chevreau C, Filipek M, Melichar B, Bajetta E, Gorbunova V, Bay JO, Bodrogi I, Jagiello-Gruszfeld A and Moore N; AVOREN Trial investigators. Bevacizumab plus interferon alfa-2a for treatment of metastatic renal cell carcinoma: a randomized, double-blind phase III trial. Lancet 2007; 370: 2103-2111.
[16] Xu YL, Chen XY, Chen X, Bian WH, Yao C, Zhu XS and Chen JJ. San Huang Decoction promotes apoptosis of breast cancer cells through regulating Aurora Kinase A. J Nanjing Univ Tradit Chin Med 2015; 31: 469-474.
[17] Xu Y, Wang C, Chen X, Li Y, Bian W and Yao C. San Huang Decoction targets Aurora Kinase A to inhibit tumor angiogenesis in breast cancer. Integr Cancer Ther 2020; 19: 1534735420983463.
[18] Zhu ZY, Xue JX, Yu LX, Bian WH, Zhang YF, Sohn KC, Shin IH and Yao C. Reducing postsurgical exudate in breast cancer patients by using San Huang decoction to ameliorate inflammatory status: a prospective clinical trial. Curr Oncol 2018; 25: e507-e515.
[19] Zhang XP, Wang C, Wang QW, Cao SH, Shao XY, Liang S, Feng M, Wang HH and Yao C. Study on the effects of SanHuang decoction on chronic stress and blood viscosity of breast cancer patients. Chinese Journal of Surgical Oncology 2020; 12: 534-538.
[20] Bian WH, Xu YL, Chen XY, Chen X, Yao C, Zhu XS, Zhang T and Gu M. SanHuang decoction regulating Aurora Kinase A and promoting epirubicine chemosensitivity on MDA-MB-231 cells. Liaoning Journal of Traditional Chinese Medicine 2016; 43: 798-803.
[21] Xu Y, Chen X, Chen X, Bian W, Yao C, Zhang X, Zhu X, Chen J and Ye X. San Huang Decoction downregulates Aurora kinase A to inhibit breast cancer cell growth and enhance chemosenstivity to anti-tumor drugs. Pathol Res Pract 2016; 212: 696-703.
[22] Feng M, Wang H, Zhu Z, Yao B, Li Y, Xue J, Cao S, Shao X, Xu Y, Sohn KC, Shin IH and Yao C. SanHuang decoction controls tumor microenvironment by ameliorating chronic stress in breast cancer: a report of ninety cases. Front Oncol 2021; 11: 677939.
[23] Chen X. San Huang decoction inhibition of PI3K/AKT signaling pathway and reduce ROS topromote MCF-7 tamoxifen-resistant cell apoptosis. Jiangsu: Nanjing University of Chinese Medicine 2017; 1-41.
[24] Chen X. Study on the mechanism of SanHuang decoction inhibiting PI3K/AKT signaling pathway in the regulation of tamoxifen resistance in breast cancer. Jiangsu: Nanjing University of Chinese Medicine 2019; 1-98.
[25] Xu B, Peng YJ, Ma BL and Cheng SD. Aberrant methylation of the 16q23.1 tumor suppressor gene ADAMTS18 promotes tumorigenesis and progression of clear cell renal cell carcinoma. Genes Genomics 2021; 43: 123-131.
[26] Xu B, Zhang L, Luo C, Qi Y, Cui Y, Ying JM, Zhang Q and Jin J. Hypermethylation of the 16q23.1 tumor suppressor gene ADAMTS18 in clear cell renal cell carcinoma. Int J Mol Sci 2015; 16: 1051-1065.
[27] Mace TA, Shakya R, Pitarresi JR, Swanson B, McQuinn CW, Loftus S, Nordquist E, Cruz-Monserrate Z, Yu L, Young G, Zhong X, Zimmers TA, Ostrowski MC, Ludwig T, Bloomston M, Bekaii-Saab T and Lesinski GB. IL-6 and PD-L1 antibody blockade combination therapy reduces tumour progression in murine models of pancreatic cancer. Gut 2018; 67: 320-332.

[28] Xu C, Fillmore CM, Koyama S, Wu H, Zhao Y, Chen Z, Herter-Sprie GS, Akbay EA, Tchaicha JH, Altabef A, Reibel JB, Walton Z, Ji H, Watanabe H, Janne PA, Castrillon DH, Rustgi AK, Bass AJ, Freeman GJ, Padera RF, Dranoff G, Hammerman PS, Kim CF and Wong KK. Loss of Lkb1 and Pten leads to lung squamous cell carcinoma with elevated PD-L1 expression. Cancer Cell 2014; 25: 590-604.

[29] Alvarez Arias DA, Kim HJ, Zhou P, Holderried TA, Wang X, Dranoff G and Cantor H. Disruption of CD8+ Treg activity results in expansion of T follicular helper cells and enhanced antitumor immunity. Cancer Immunol Res 2014; 2: 207-216.

[30] Szturz P and Vermorken JB. Immunotherapy in head and neck cancer: aiming at EXTREME precision. BMC Med 2017; 15: 110.

[31] Xu H, Xiao Q, Fan Y, Xiang T, Li C, Li C, Li S, Hui T, Zhang L, Li H, Li L and Ren G. Epigenetic silencing of ADAMTS18 promotes cell migration and invasion of breast cancer through AKT and NF-κB signaling. Cancer Med 2017; 6: 1399-1408.

[32] Lu T, Dang S, Zhu R, Wang Y, Nie Z, Hong T and Zhang W. Adamts18 deficiency promotes colon carcinogenesis by enhancing β-catenin and p38MAPK/ERK1/2 signaling in the mouse model of AOM/DSS-induced colitis-associated colorectal cancer. Oncotarget 2017; 8: 18979-18990.